Numerical evaluation of an innovative cup layout for open volumetric solar air receivers

Numerical evaluation of an innovative cup layout for open volumetric solar air receivers

Mattia Cagnoli, Laura Savoldi, Roberto Zanino, and Fritz Zaversky

Citation: AIP Conference Proceedings **1734**, 030007 (2016); doi: 10.1063/1.4949059
View online: http://dx.doi.org/10.1063/1.4949059
View Table of Contents: http://scitation.aip.org/content/aip/proceeding/aipcp/1734?ver=pdfcov
Published by the AIP Publishing

Numerical Evaluation of an Innovative Cup Layout for Open Volumetric Solar Air Receivers

Mattia Cagnoli[1], Laura Savoldi[1, a)], Roberto Zanino[1] and Fritz Zaversky[2]

[1]*Dipartimento Energia, Politecnico di Torino, C.so Duca degli Abruzzi 24, 10129 Torino, Italy*
[2] *National Renewable Energy Center (CENER), Solar Thermal Energy Department, Sarriguren (Navarra), Spain*

[a)] laura.savoldi@polito.it

Abstract. This paper proposes an innovative volumetric solar absorber design to be used in high-temperature air receivers of solar power tower plants. The innovative absorber, a so-called CPC-stacked-plate configuration, applies the well-known principle of a compound parabolic concentrator (CPC) for the first time in a volumetric solar receiver, heating air to high temperatures. The proposed absorber configuration is analyzed numerically, applying first the open-source ray-tracing software Tonatiuh in order to obtain the solar flux distribution on the absorber's surfaces. Next, a Computational Fluid Dynamic (CFD) analysis of a representative single channel of the innovative receiver is performed, using the commercial CFD software ANSYS Fluent. The solution of the conjugate heat transfer problem shows that the behavior of the new absorber concept is promising, however further optimization of the geometry will be necessary in order to exceed the performance of the classical absorber designs.

INTRODUCTION

Volumetric solar receivers are typically used at central receiver plants in order to heat a gaseous fluid (usually the ambient air) to high temperatures. A volumetric receiver can either work at ambient pressure, in which case it is called an open volumetric receiver, or in pressurized mode, where the high pressure gas stream is heated through a transparent quartz window. The former approach (non-pressurized) is typically applied at central receivers driving Rankine steam cycles [1], while the latter approach (pressurized) is used for solar powered Brayton cycles [2-5].

The present work is based on the experience obtained by the SOLAIR [6] and HiTRec [7] projects, where the absorber design relied on the honeycomb concept, consisting of small parallel prismatic channels. Our work focuses on the numerical evaluation of a high-temperature open volumetric solar air receiver, made of a ceramic material, siliconized silicon carbide (SiSiC). We propose an innovative volumetric absorber design, consisting of a series of identical plates (see Fig. 1), each one including parabolic profiles and triangular elements, combining the compound parabolic concentrator (CPC) geometry [8] with the concept of a cone beam dump [9], in order to obtain deeper solar flux invasion. This should lead to higher thermal efficiencies thanks to an improved "volumetric effect", i.e. the situation where the outlet air temperature is higher than the solid temperature at the inlet [10], compared to the conventional absorber design. (Note that the realization and implications of the volumetric effect have still to be proved at experimental level.) The conventional design was analyzed in a previous study [11] applying the same methodology as used in the present paper, thus enabling a direct comparison between the conventional and the proposed innovative absorber layout.

With reference to Fig. 1, in this paper we focus on the analysis of a single-channel. The cup and the receiver levels will be addressed in future work.

The analysis is divided into two steps:

1. Using the Tonatiuh ray-tracing software [12] and the optical properties of the ceramic material, the distribution of the absorbed photons on the receiver's surfaces is determined. Starting from the data of the

SolarPACES 2015
AIP Conf. Proc. 1734, 030007-1–030007-8; doi: 10.1063/1.4949059
Published by AIP Publishing. 978-0-7354-1386-3/$30.00

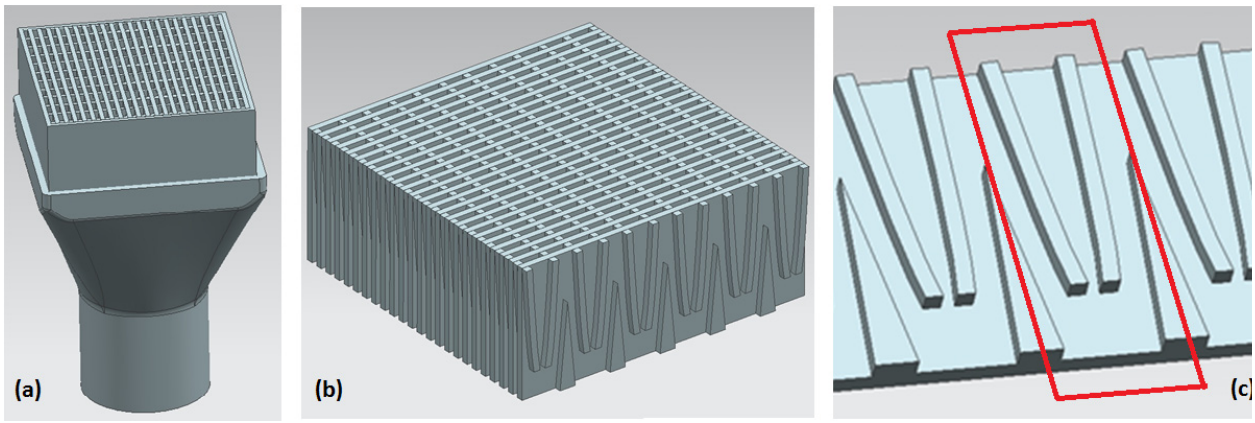

FIGURE 1. Receiver cup (a), the innovative absorber (b), one single plate of the absorber (c) with a "single channel" highlighted by the red rectangle.

optic analysis, the distribution of the absorbed heat flux on the inner surface of a single channel is computed, providing the driver for the thermal-fluid dynamic simulation in the second step.

2. Computational Fluid Dynamic (CFD) analysis of a single channel, using the commercial CFD software ANSYS Fluent, is performed to solve the conjugate heat transfer problem. The analysis is aimed at assessing the level of volumetric effect reached in the channel, as well as at the thermal-hydraulic characterization of the single channel, which will be eventually useful for the CFD analysis of the cup.

OPTICAL ANALYSIS AND EVALUATION OF THE ABSORBED HEAT FLUX DISTRIBUTION

The optical analysis requires the simulation of a small representative section of a solar power tower plant, consisting of a heliostat field section and a corresponding portion of the whole receiver, in order to determine the photon absorption and scattering on the surfaces of interest. The layout of the system adopted in the analysis is shown in Fig. 2a. The analysis has been performed using the open-source ray-tracing software Tonatiuh [12, 13].

The heliostat field is rectangular-shaped and consists of 110 spherical tracking mirrors, arranged in 10 rows and 11 columns. It corresponds to the portion of the whole heliostat field that aims at a specific aiming point, around which the portion of the receiver is placed. Each heliostat measures 5x5 meters and the free space between two adjacent mirrors is set equal to 0.5 meters, the radius of curvatures instead changes from heliostat to heliostat in order to ensure that the focal point is always coincident with the aiming point: the center of the irradiated face of the absorber tested. Regarding the optical properties, it is assumed a reflectivity equal to 100%, and we consider a fixed value of the slope deviation equal to 3.5 mrad [14].

The receiver section considered in Tonatiuh is a square-shaped grid of 69 channels (23 rows and 3 columns). The axis of the channels is tilted by 53° with respect to the horizontal as shown in Fig. 2c, in order to minimize the sum of the incident angles and so to optimize the penetration of solar rays and the absorbed heat, according to Lambert's cosine law. It should be noted that the resulting minimum-incidence-angle tilt depends on the specific tower height and solar field configuration and is thus only valid for the chosen simulation setup. For a detailed explanation the interested reader is referred to Ref. [15]. A view of the receiver from the Tonatiuh GUI is provided in Fig. 2b, while Fig. 2d illustrates the single channel dimensions.

The siliconized silicon carbide (SiSiC) properties assumed in the present paper are summarized in Table 1. The absorber material is considered in Tonatiuh as if it were a specular behaving material. That is, the absorber plates are assumed to be hard machined (grinded) after sintering, such that their optic behavior is for a large part specular. However, a fully specular behavior is definitely an idealization, which is justified here only to the purpose of demonstrating the theoretical ideal behavior of the proposed geometry.

TABLE 1. Summary of the relevant physical properties of SiSiC

Parameter	Value
Solar absorptivity [16]	0.8
Solar absorptivity (with selective coating – Case III – front face)	0.9
Solar absorptivity (with selective coating – Case III – inner walls)	0.6
Thermal emissivity @ 1100 ºC [17]	0.8
Thermal emissivity (with selective coating – Case III)	0.4
Thermal conductivity @ 1000 ºC (W/m·K) [18]	40
Upper temperature limit (ºC) [19]	1400

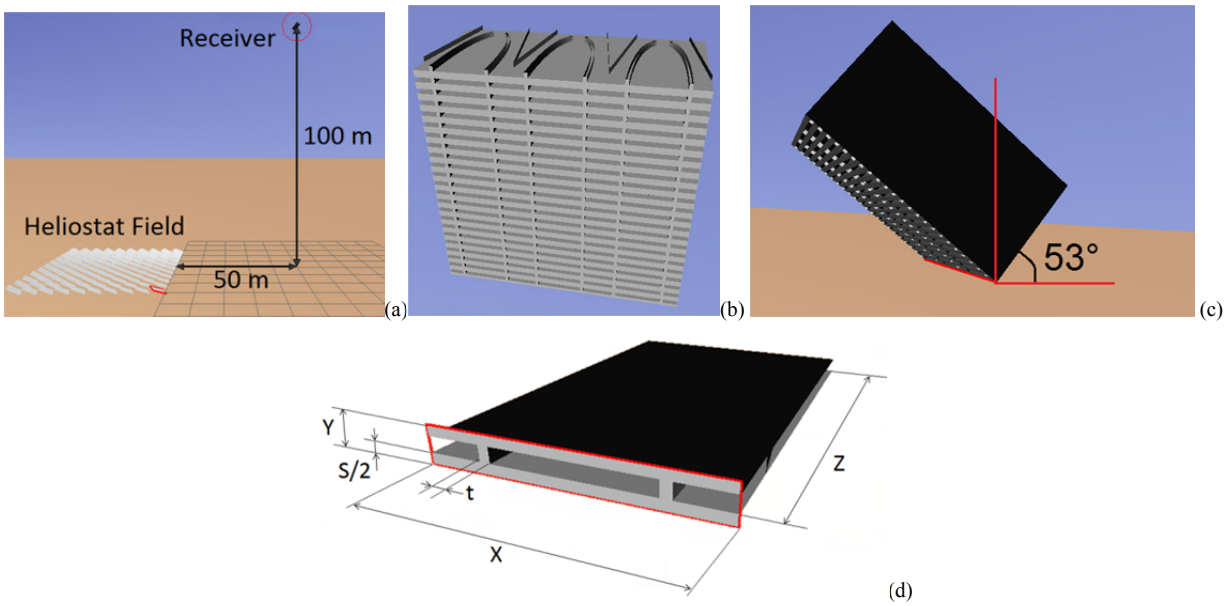

FIGURE 2. Overview of the simulated system in Tonatiuh, with the receiver oversized to make it visible (a); tested absorber (b); tilt angle (c); and single channel with geometric details (d): $X = 0.027$ m, $Y = 0.0035$ m, $Z = 0.042$ m, $t = 0.001$ m, $s = 0.002$ m

The sun position has been set as on 21st of June, at noon, at latitude 35.5º and longitude -5.23 º (near Tétouan, Morocco). The number of photons simulated with the Monte Carlo code is set equal to 1 billion, which we checked is large enough to give a solar flux distribution on the absorber's surfaces independent of the chosen number of photons.

The computed data about the photon absorption and scattering on the receiver surfaces (Tonatiuh output) are then post-processed with a Matlab code in order to generate the heat flux maps reported in Fig. 3. The reference frame of the heat flux maps is defined such that the *z* axis corresponds to the longitudinal axis of the channel, pointing in the direction of air flow, the *x* axis is parallel to the absorber's plate, pointing towards the right-hand side when seeing the channel from the front, and the *y* axis is normal to the absorber's plate and points upwards (see Fig. 2d). The origin of the axes is located at the outlet pupil of the CPC at the channel's center.

Figs. 3a and b show that the cathedral-glass pattern of the absorbed heat flux on the horizontal surfaces of the channel decreases from the inlet and is obviously larger for the ceiling of the channel than for the floor, because of the value chosen for the tilt angle. In Fig. 3c it is shown that the heat flux on the frontal face is more or less uniform, with relative variations of less than ± 10%; this is because the irradiated frontal area of the assumed receiver is too small to appreciate changes in the incident power when moving away from the aiming point, which is at the center of the face. The most interesting outcome from the post-processing of the optical data is however the heat flux trend along the CPC's internal face (blue line in Fig. 3d). It demonstrates that the parabolic profile works correctly, focusing the solar radiation in a deeper section of the channel: the exit pupil of the CPC trough. Conversely, all the other inner surfaces absorb the major part of the incoming power close to the inlet section.

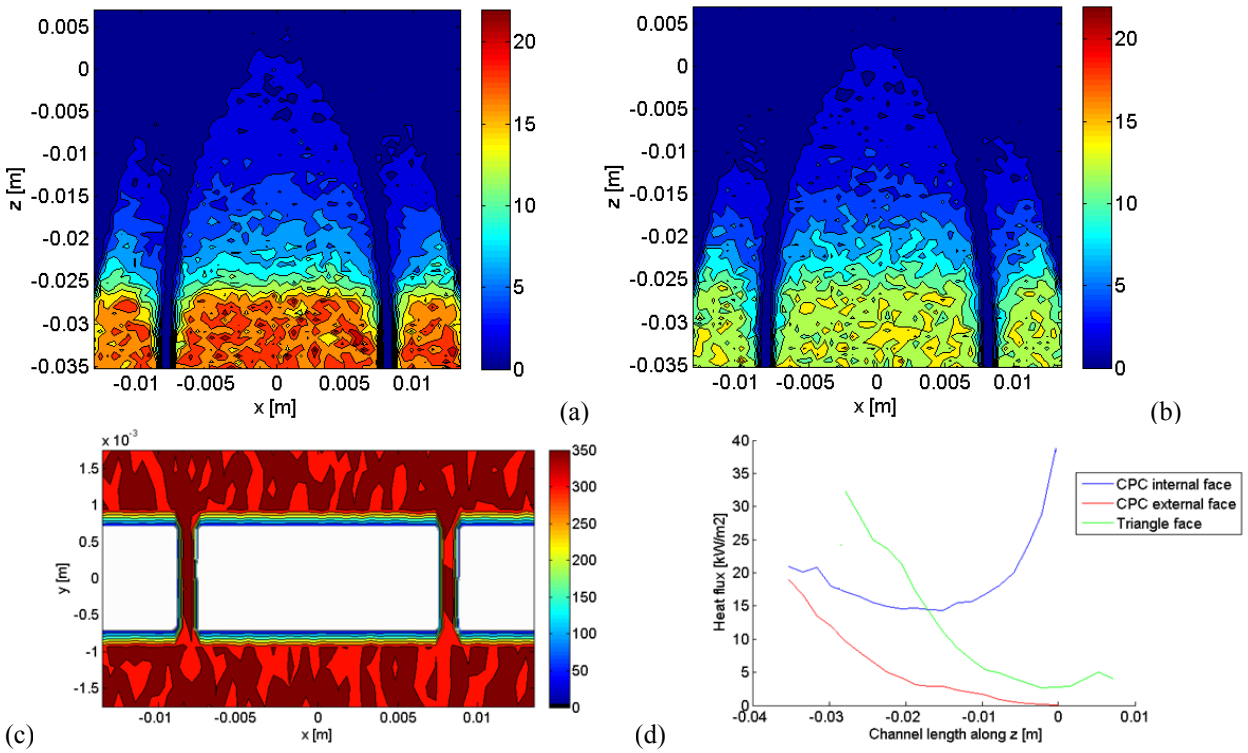

FIGURE 3. Computed absorbed heat in kW/m^2 on the different surfaces of a single channel: (a) ceiling; (b) floor; (c) frontal face; (d) internal vertical faces in contact with the air stream

THERMAL FLUID DYNAMIC ANALYSIS

The CFD analysis is initially performed at the single-channel level, with the aim to evaluate the receiver's efficiency and to check if the volumetric effect occurs. The volumetric effect (VE) is defined as the situation where the air outlet temperature ($T_{\text{air out}}$) is higher than the temperature of the solid structure at the inlet section ($T_{\text{solid in}}$). To quantify this effect we introduce the parameter

$$\Delta T_{VE} = T_{air\ out} - T_{solid\ in}\,. \tag{1}$$

The receiver efficiency

$$\eta = \frac{P_{air}}{P_{in}} = \frac{P_{abs}}{P_{in}} \cdot \frac{P_{air}}{P_{abs}} = \eta_{optic} \cdot \eta_{th} \tag{2}$$

is defined as the ratio between the power gained (P_{air}) by the fluid stream and the incident solar power (P_{in}) and it can be split in two terms: the optical efficiency (η_{optic}) and the thermal efficiency (η_{th}). The optical efficiency includes the losses due to the photon reflection, i.e. it takes into account how the receiver is able to absorb photons, out of all the photons impinging on it. The thermal efficiency takes into account the heat transfer phenomena (conduction, convection and radiation), i.e. it measures how well the receiver is able to transfer the absorbed solar energy to the air stream.

Thanks to the symmetry in the channel geometry, only half of the whole structure is numerically investigated, as shown in Fig. 4. ANSYS Fluent® models the conjugate heat transfer problem of our interest with the following set of coupled equations:

- Hydraulic model: steady-state 3D incompressible Navier-Stokes equations;

- Thermal model: steady-state 3D energy equations both for the fluid and solid domain;
- Radiative model: Radiative heat transfer equation between inner walls and between the inner walls and the external ambient (so-called surface-to-surface model – *s2s* [20]).

The boundary conditions are defined as follows: at the inlet, two different velocities are set, one for the inlet section of the CPC trough and the other one for the aperture on the triangle side. The two velocities were chosen such that the pressure difference between the two inlets is negligible (see Fig. 5b) and the area-weighted average velocity is equal to 0.47 m/s, which is the mean velocity measured during the SolAir 200 experiment [6]. A fixed value of pressure is set for the outlet section. As it can be deduced from Fig. 5a, the air velocity in the channel is sufficiently low to justify the assumption of laminar, incompressible flow. In fact, the Reynolds number, calculated in the section with the smallest wetted perimeter, is less than 100, while the Mach number is ~ 0.003.

The thermal boundary conditions have been set such that the channel's inner surfaces in contact with the air flow (triangle face, CPC internal and external side, ceiling and floor plates) have an imposed heat flux distribution according to the results of the optical analysis (see Fig. 3). To set a specific trend for each face, a UDF (User Defined Function) was written. The surfaces in contact with adjacent channels have been defined as adiabatic, as well as the back side of the absorber, thus ensuring symmetry conditions with respect to the neighboring channels, as well as no heat loss at the rear of the absorber, respectively. Finally, a uniform heat flux is applied on the frontal face of the absorber (as the relative variations in heat flux are rather small; see Fig. 3c) and a convective and radiative heat-loss boundary condition towards the ambient air is defined. In particular, for the convective share, a

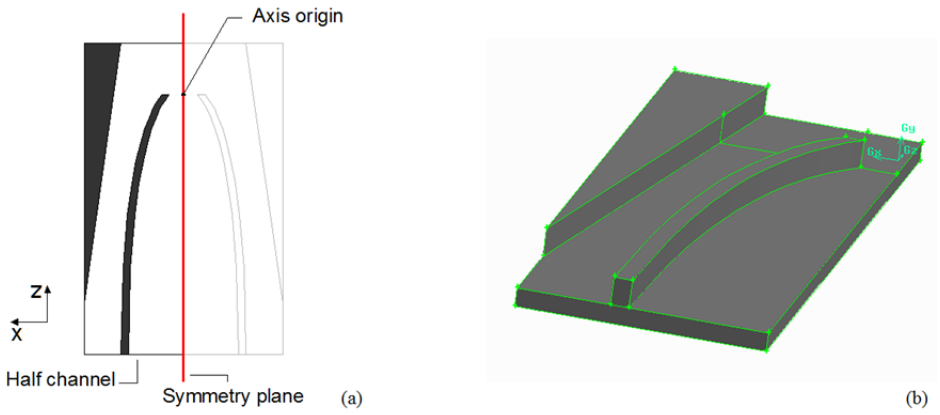

FIGURE 4. 2D view of the channel with the symmetry plane (a); 3D view of the computational domain without the ceiling (b).

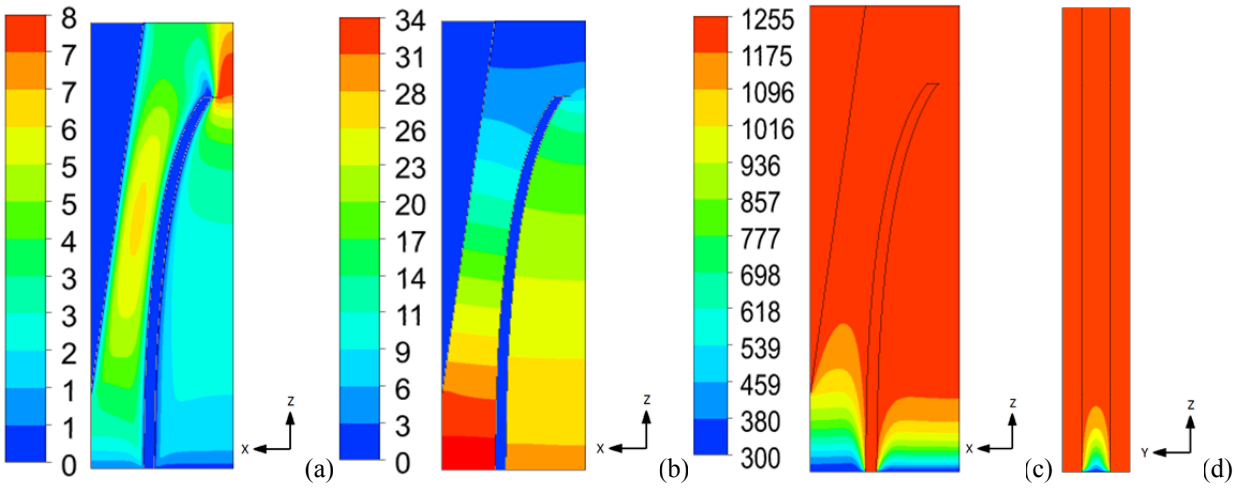

FIGURE 5. Computed results: (a) air speed (m/s); (b) air overpressure with respect to outlet (Pa); (c, d) temperature (K). Maps on the horizontal midplane (a, b, c) and on the vertical symmetry plane of Fig. 4 (d), respectively.

TABLE 2. Summary of the computed global parameters of receiver performance and comparison to the conventional design

	Innovative CPC-stacked-plate design			Conventional honeycomb [11]
	Case I (s = 2 mm)	**Case II (s = 0.8 mm)**	**Case III (s = 0.8 mm + surface coatings)**	
$T_{\text{air out}}$ (K)	1250	1103	1133	1046
$T_{\text{solid in}}$ (K)	1214	1024	1043	1052
$T_{\text{solid out}}$ (K)	1250	1103	1132	1046
η (%)	50.4	64.2	66.9	69.6
η_{optic} (%)	85.9	88.9	90.7	93.4
η_{th} (%)	58.7	72.2	73.8	74.5
ΔT_{VE} (K)	36	79	90	-6
$\eta_{overall}$ (%)	38.3	46.7	49.2	49.6

heat transfer coefficient of 10 W/(m^{2}K) is assumed (Solar Two [21]). A sensitivity analysis was performed doubling and halving this value; results indicate that the convective heat losses from the front face don't have a significant influence on the absorber's performance. Regarding the radiative share, the thermal emissivity of the receiver's front is set to 0.8. The ambient temperature is set to 300 K, for both the convective and the radiative heat transfer as well as for the air entering the channel.

The computed results are reported in Fig. 5: in Fig. 5a we notice the acceleration-deceleration pattern of the air flow field, corresponding to the change in the channel cross section; the more-or-less 1D linear decrease of the pressure along the channel is reported in Fig. 5b; the progressive increase of the air temperature from the inlet and the roughly uniform temperature profile in the solids are reported in Figs. 5c, d. These results can be post-processed to obtain the key parameters, globally characterizing the receiver performance, according to the above-mentioned definitions (see Eq. 1 and 2).

Table 2 displays the obtained global performance indicators for 3 design iterations (Cases I, II and III, respectively) of the innovative CPC-stacked-plate absorber as well as for the conventional honeycomb absorber that was analyzed in a previous work [11] using the same methodology. Note that the comparison between the innovative and the conventional absorber design is made based on the boundary condition of equal channel inlet velocity, which means that for a specific thermal power at receiver level (macro scale) a different number of channels, i.e. cups must be considered.

Case II differs from Case I in that the plate thickness s is reduced to 0.8 mm in order to reduce the frontal frame area of the absorber, which decreases the photon reflection as well as the radiative and convective heat losses from the front face. In the basic configuration (Case I) 60% of the front face of the single channel is covered by the solid frame, whereas in Case II only 40% of the front face is covered by the solid frame. Case III differs from Case II in that surface coatings are introduced. In particular, in Case III we apply a solar selective coating at the receiver's front face, as already widely applied at solar collectors for lower temperatures. However, there is a need to develop selective absorber coatings that are suitable for much higher working temperatures (at or above 1000 ºC) and that are furthermore stable under air [22], which are current topics of research [23]. Therefore, reasonable selective coating properties (a solar absorptance of 90% and thermal emittance of 40% at 1000 ºC) are assumed, which will be most likely achieved within the next years. Furthermore, an increased reflectivity of the channel's internal surfaces is assumed in Case III (for all inner surfaces except for the CPC profile), which leads to an enhanced reflection of the solar rays and thus a deeper solar flux invasion that is important in order to move the bulk of the solar flux absorption as deep as possible into the channel, avoiding high temperatures at the entrance. Recent research in the area of plasma-sprayed coatings [24] enables an almost arbitrary adjustment of the reflectivity. In Case III it was set to 0.4 instead of 0.2 as used in Case I and II.

As can be seen from the results in Table 2, the basic configuration (Case I) has a rather weak performance when compared to the conventional honeycomb (η ~ 50% vs. 70%), which is likely mainly due to the bigger share of the frontal face of the absorber covered by solid structure (60% vs. 21%), which increases the photon reflection to the outside as well as the radiative and convective heat losses. Indeed, by reducing this share of the solid structure down to 40% (Case II), the optical as well as the thermal receiver efficiency improve notably, increasing the receiver efficiency by ~14 percentage points to ~ 64%. By additionally applying advanced surface coatings, the receiver

efficiency is further increased by roughly 3 percentage points reaching ~67%, however still remaining below the conventional receiver's performance of 69.6% efficiency. On the other hand, the outlet temperature increases compared to the conventional setup and the so-called "volumetric effect" occurs (positive values of ΔT_{VE}), whilst in the conventional design it was not achieved, and the expected correlation between the volumetric effect and the receiver efficiency is observed for the innovative absorber design. However, the increase in temperature is outperformed by the reduction in receiver efficiency η, as highlighted by the fact that the overall efficiency

$$\eta_{overall} = \eta \cdot \eta_{Carnot} \tag{3}$$

barely reaches that of the conventional honeycomb design, see Table 2. The small efficiency gap that can be still observed may be due to:

- A still relatively high share of the solid structure on the frontal absorber face, causing higher radiative as well as convective heat losses.
- A significantly lower ratio of available heat transfer area per channel inlet cross-sectional area. In fact, the standard setup has almost twice as much specific heat transfer area than the innovative setup. The conventional honeycomb has 100 m^2 of heat transfer area for each square meter of channel inlet cross-sectional area. On the contrary, the innovative CPC-stacked-plate absorber in its current configuration has only 56 m^2 of heat transfer area per square meter of channel inlet area. This is a principle limitation of the new design and we will work to improve on this in the future.

CONCLUSIONS AND PERSPECTIVE

This paper proposes an innovative design for a volumetric solar absorber to be used in high-temperature air receivers of solar power tower plants. The innovative absorber, a so-called CPC-stacked-plate configuration, applies the well-known principle of a compound parabolic concentrator (CPC) [8] for the first time in a volumetric solar receiver, heating air to high temperatures. Additionally, the CPC concept is combined with the concept of a cone beam dump, in order to trap the solar rays deep in the absorber structure, with the objective to move the bulk of the solar flux absorption as deep as possible into the channel, i.e. avoiding high temperatures at the entrance, thus enhancing the volumetric effect.

It has been shown numerically that the innovative absorber geometry can achieve the volumetric effect under theoretical ideal conditions, unlike the conventional honeycomb design, thanks to the fact that the CPC trough between the parallel plates successfully focuses the solar energy at the rear pupil. However, for the remaining surfaces, which represent the most part of the geometry, the bulk of the solar flux is still absorbed close to the channel's entrance, limiting its thermal performance. Additionally, a relatively high share of frontal solid surface increases the back reflection of photons as well as the radiative and convective heat losses, and the specific heat transfer area (per unit frontal area) is almost half of the value obtained with conventional honeycombs.

Nevertheless, there is much room for improvements, mainly on the geometric part of the absorber design, aiming at a higher specific heat transfer area, a lower share of solid at the frontal face and obviously a bigger share of CPC surface within the channel. In this context, the actual benefit of including a cone beam dump in the structure shall be investigated, in comparison to a full-CPC layout. It is clear that future work must focus on the optimization of the proposed absorber concept, working closely with experts in manufacturing of high-temperature ceramics. It is very likely that the optimized configuration will exceed the conventional design in optical and thermal performance. In order to also confirm the performance at the macro scale, the present analysis will have to be extended to the cup level and then to the full-receiver level.

ACKNOWLEDGMENTS

The contribution of Dr. Fritz Zaversky has received funding from the European Union's Seventh Framework Programme, under grant agreement No 608593 (EUROSUNMED), as well as from the project MIRASOL, ref ENE2012-39385-C03-01 (CENER), within the framework "Subprograma de Proyectos de Investigación Fundamental no orientada (2012)", MINECO (Spanish Government).

REFERENCES

1. K. Hennecke, B. Hoffschmidt, G. Koll, P. Schwarzbözl, J. Göttsche, M. Beuter and T. Hartz, "The solar power tower Jülich - A solar thermal power plant for test and demonstration of air receiver technology", Beijing, China, 2007
2. W. E. C. Pritzkow, Solar Energy Materials **24** (1–4), 498-507 (1991).
3. J. Karni, R. Rubin, D. Sagie, A. Fiterman, A. Kribus and P. Doron, Journal of Solar Energy Engineering **119** (1), 74-78 (1997).
4. R. Buck, M. Pfänder, P. Schwarzbözl, F. Tellez, T. Bräuning and T. Denk, Journal of Solar Energy Engineering **124** (1), 2-9 (2002).
5. P. Heller, M. Pfänder, T. Denk, F. Tellez, A. Valverde, J. Fernandez and A. Ring, Solar Energy **80** (10), 1225-1230 (2006).
6. F. Téllez, "Thermal performance evaluation of the 200kWth "SolAir" volumetric solar receiver", CIEMAT-PSA, Madrid, Spain, 2003
7. B. Hoffschmidt, F. l. M. Téllez, A. Valverde, J. s. Fernández and V. Fernández, Journal of Solar Energy Engineering **125** (1), 87-94 (2003).
8. R. Winston, Solar Energy **16** (2), 89-95 (1974).
9. P. C. D. Hobbs, *Building electro-optical systems: Making it all work*, 2nd Edition ed. (Wiley, New York, USA, 2009).
10. M. Romero, R. Buck and J. E. Pacheco, Journal of Solar Energy Engineering **124** (2), 98-108 (2002).
11. L. Bergamasco, F. Zaversky, R. Bonifetto, L. Savoldi and R. Zanino, "Preliminary Numerical Evaluation of Advanced Open Volumetric Solar Receiver Designs Counteracting Non-Ideal Volumetric Behavior", presented at SolarPACES Beijing, China, 2014
12. M. J. Blanco, J. M. Amieva and A. Mancilla, "The Tonatiuh Software Development Project: An Open Source Approach to the Simulation of Solar Concentrating Systems", Orlando, Florida, 2005
13. M. J. Blanco, A. Mutuberria and D. Martinez, "Experimental Validation of Tonatiuh using the Plataforma Solar de Almería Secondary Concentrator Test Campaign Data", Perpignan, France, 2010
14. G. Johnston, Journal of Solar Energy Engineering **117** (4), 294-296 (1995).
15. M. Cagnoli, "Numerical evaluation of an innovative open-volumetric air receiver layout in the context of solar power tower plants, MSc Thesis", Politecnico di Torino, Turin, Italy, 2015
16. R. Pitz-Paal, J. Morhenne and M. Fiebig, Solar Energy Materials **24** (1–4), 293-306 (1991).
17. E. Sani, L. Mercatelli, D. Jafrancesco, J. L. Sans and D. Sciti, Journal of the European Optical Society **7** (2012).
18. FCT-Keramik, "Silicon Carbide Materials and Components", FCT Hartbearbeitungs GmbH, Sonneberg, Germany, 2015
19. A. L. Ávila-Marín, Solar Energy **85** (5), 891-910 (2011).
20. ANSYS-Inc., "ANSYS Fluent Theory Guide", ANSYS Inc., Canonsburg, USA, 2013
21. C. K. Ho and B. D. Iverson, Renewable and Sustainable Energy Reviews **29**, 835-846 (2014).
22. C. Kennedy, "Review of mid- to high-temperature solar selective absorber materials", NREL - National Renewable Energy Laboratory, Golden, Colorado, USA, 2002
23. A. Soum-Glaude, I. Bousquet, L. Thomas and G. Flamant, Solar Energy Materials and Solar Cells **117** (0), 315-323 (2013).
24. J. Marthe, E. Meillot, G. Jeandel, F. Enguehard and J. Ilavsky, Surface and Coatings Technology **220** (0), 80-84 (2013).